Electrochemical activation of oblique angle deposited Cu catalyst film for H2 production

Journal:	*Catalysis Science & Technology*
Manuscript ID:	CY-ART-11-2014-001524.R3
Article Type:	Paper
Date Submitted by the Author:	07-Jan-2015

Complete List of Authors:	Antonio, de Lucas; University of Castilla La Mancha, Gonzalez Cobos, Jesus; University of Castilla La Mancha, Chemical Engineering Rico, Victor; Consejo Superior de Investigaciones Cient&#65533;ficas (CSIC), Instituto de Ciencia de Materiales de Sevilla Gonzalez-Elipe, Agustin; Consejo Superior de Investigaciones Cient&#65533;ficas (CSIC), Instituto de Ciencia de Materiales de Sevilla Valverde, José; University of Castilla-La Mancha, Chemical Engineering

Journal Name Catalysis Science & Technology Dynamic Article Links ►

Cite this: DOI: 10.1039/c0xx00000x

www.rsc.org/xxxxxx

ARTICLE TYPE

Electrochemical activation of oblique angle deposited Cu catalyst film for H_2 production

Jesús González-Cobos,[a] Víctor J. Rico,[b] Agustín R. González-Elipe,[b] José L. Valverde[a] and Antonio de Lucas-Consuegra*[a]

Received (in XXX, XXX) Xth XXXXXXXXX 20XX, Accepted Xth XXXXXXXXX 20XX
DOI: 10.1039/b000000x

A novel Cu catalyst film was prepared by oblique angle physical vapour deposition (OAD) on a K-βAl_2O_3 solid electrolyte (alkaline ionic conductor) for catalytic/electrocatalytic purposes. This technique allowed to obtain a highly porous and electrically conductive Cu catalyst electrode which was tested in the partial oxidation of methanol (POM) reaction for H_2 production and its catalytic activity was in-situ enhanced via electrochemical promotion of catalysis (EPOC). The electropromotional effect was reversible and reproducible, and allowed to increase both hydrogen and methyl formate production rates by almost three times under optimal promotion conditions (320 ºC, 2.2 x 10^{-7} mol K^+ transferred). The observed promotional effect was attributed to a decrease of the Cu catalyst work function as a consequence of the controlled migration of electropositive K^+ ions which favoured the chemisorption of electron acceptor molecules (O_2) at the expense of the electron donor ones (CH_3OH). Under reaction conditions these ions formed some kind of potassium surface compounds as demonstrated by SEM, EDX and XPS post-reaction characterization analysis. The obtained results demonstrate the interest of the used catalyst-electrode preparation technique for the electrochemical activation of non-noble metal catalyst films.

Introduction

Alkali ions have been widely employed as promoters of metal catalysts to modify their activity and selectivity. In this sense, the electrochemical promotion of catalysis (EPOC) is a straightforward technique to study the effect of electronic promoters on the reaction rate.[1] The EPOC phenomenon is based on the electrochemical pumping of promoter ions from a solid electrolyte support to the catalytically active metal film.[1] Hence, while the conventional catalytic promotion is carried out by adding a specific amount of promoter during the preparation step of the catalyst, in the case of the electrochemical promotion, the electrically induced back-spillover of promoter species enables to in-situ control and enhance the catalytic performance of the catalyst film during the reaction step.[2] This phenomenon has been applied with a large variety of catalysts and solid electrolytes (cationic, anionic or mixed conductors) in a wide variety of catalytic reactions of industrial and environmental interest.[3] Nowadays, some of the main challenges of EPOC for further technological progress are the design of scaled-up reactors and material cost minimization. With regard to the former, increasingly more compact and efficient reactors designs based, for example, on monolithic configurations or hollow fibre membranes can be found in literature.[4-8] Several EPOC studies have also dealt with the improvement of catalytic materials and the development of electrodes consisting of catalysts highly dispersed on gold,[9] mixed ionic electronic conductors,[10] carbonous materials[11-13] and yttria-stabilized zirconia (YSZ),[14-17] or catalysts based on non-noble (lower cost) metals such as Ni,[11, 18-21] Fe[4, 22, 23] or Cu[7, 24-27]. A summary of these works along with the studied catalytic reaction in each case is reported in Table 1.

Important features of these metallic catalyst films such as their porosity, surface area or metal dispersion strongly depend on the preparation method. Different techniques have been used in EPOC studies for the preparation of the active catalyst film such as: deposition and calcination of an organometallic paste,[4, 17, 20, 22] impregnation of a metal precursor solution,[9, 10, 18] spray deposition in a carbon matrix[12] or other less conventional techniques which enable a better control of the microstructure of the film, including Physical Vapour Deposition (PVD) methods such as sputtering,[5-7, 14, 24, 25] Cathodic Arc Deposition (CAD)[13] or Pulsed Laser Deposition (PLD).[28] In the present work, we propose for the first time in literature a modification of the PVD technique called Oblique or Glancing Angle Deposition (OAD or GLAD) for the preparation of the film. By this method the substrate is placed in an oblique or glancing angle configuration with respect to the evaporated flux of deposition material to enhance the shadowing effects during the film growth.[29] As a result, highly porous films formed by tilted nanocolumns are obtained, which are characterized by a high gas-exposed surface area and a controlled microstructure depending on the vapour incident angle, the rotation speed of the substrate, and the temperature during the deposition, among other factors. The open

Cite this: DOI: 10.1039/c0xx00000x

www.rsc.org/xxxxxx

ARTICLE TYPE

Table 1 Most relevant EPOC studies in the search for scale-up reactors and material cost minimization.

Efficient and compact reactor designs

Reactor configuration	Electrochemical catalyst	Reaction under study	Ref.
Multi-pellet configuration	$Fe/CaIn_{0.1}Zr_{0.9}O_{3-\alpha}$	NH_3 synthesis	4
Monolithic electropromoted reactor (MEPR)	Rh/YSZ/Pt	C_2H_4 oxidation and NO reduction by C_2H_4 in presence of O_2	5,6
	Cu-TiO_2/YSZ	CO_2 hydrogenation	7
Hollow fibre membranes	Pt/LSCF	C_2H_4 oxidation	8

Highly dispersed electrochemical catalysts

Electrochemical catalyst [a]	Reaction under study	Ref.
Pt-Au/YSZ	C_2H_4 oxidation	9
Pt-LSCF-GDC/GDC	C_3H_8 oxidation	10
Ni-CNF/YSZ	CO_2 hydrogenation	11
Ru-CNF/YSZ		
Pt-C/K-βAl_2O_3	CO and C_3H_6 oxidation	12
Pt-DLC/K-βAl_2O_3	CH_3OH partial oxidation	13
	CH_3OH steam reforming	
Au-YSZ/K-βAl_2O_3	CH_3OH partial oxidation	14
Pt/YSZ	NO reduction by C_3H_6	15
Pd/YSZ	CH_4 oxidation	16
(honeycomb monolith)		
Pt-YSZ/Na-βAl_2O_3	CH_4 steam reforming	17
	CH_4 partial oxidation	
	CH_4 autothermal reforming	

Non noble metal catalysts

Electrochemical catalyst [a]	Reaction under study	Ref.
Ni/K-βAl_2O_3	Water-gas shift	18
$Ni/CsHSO_4$	C_2H_4 hydrogenation	19
Ni/YSZ (solid oxide fuel cell)	CH_4 steam reforming	20
Ni-CNF/YSZ	CO_2 hydrogenation	11
Ni/YSZ (tubular reactor)	CO_2 hydrogenation	21
Fe/$K_2YZr(PO_4)_3$	NH_3 decomposition	22
Fe/SZY	NH_3 synthesis	23
$Fe/CaIn_{0.1}Zr_{0.9}O_{3-\alpha}$	NH_3 synthesis	4
(multi-pellet reactor)		
Cu/Na-βAl_2O_3	NO reduction by CO	24,25
PtCu/Nafion (PEM fuel cell)	PROX, water-gas shift	26
Cu-TiO_2/YSZ	CO_2 hydrogenation	7
(monolithic reactor)		
Cu/ K-βAl_2O_3 (tubular reactor)	CO_2 hydrogenation	27

[a] Unless otherwise stated, the employed reactor presented a single pellet configuration.

porosity of these films is very useful to prepare host materials for devices with optical, photonic or magnetic applications[30, 31] or for the development of gas and liquid sensors.[29] They have also been used for different energy related applications including photoelectrochemical cells,[29] solid-state hydrogen storage[32] and electrocatalysis for oxygen reduction in polymer electrolyte membrane fuel cells[33] and 2-propanol oxidation in alkaline direct alcohol fuel cells.[34]

In the present study, a novel Cu electrode prepared by OAD with both suitable catalytic and electrical properties has been applied in the electrochemical promotion of the partial oxidation of methanol (POM) reaction. This exothermic reaction is especially interesting for on board H_2 production due to the liquid nature of methanol, its high H/C ratio and its availability from a wide variety of sources. The selection of a Cu catalyst is justified by its lower cost in comparison with noble metals such as Pt or Pd and its proven catalytic activity for the POM reaction.[35-39] For this selection we have also taken into account previous works showing the suitability of Cu-based catalysts to study fundamental aspects of the EPOC phenomenon[40] and its application in different catalytic reactions such as NO reduction by CO,[24, 25] preferential oxidation of CO[26] and CO_2 hydrogenation.[7, 27] However, to the best of our knowledge, this is the first time that this non-noble metal catalyst is electrochemically promoted in a H_2 production reaction.

Experimental

Electrochemical catalyst preparation

The electrochemical catalyst consisted of a continuous thin Cu layer (geometric area of 2.01 cm^2), which also behaved as working electrode (W), deposited on one of the sides of a 19-mm-diameter, 1-mm-thick K-βAl_2O_3 (Ionotec) pellet which was used as cationic solid electrolyte (i.e. as source of K^+ promoter ions). In first place, inert Au counter (C) and reference (R) electrodes were prepared on the other side of the electrolyte by applying thin coatings of gold paste (Fuel Cell Materials 233001) followed by calcination at 800 ºC for 2 h (heating ramp of 5 ºC/min). Then, the active Cu catalyst/working electrode film was deposited by evaporation of a Cu target (Goodfellow, 99.9999 % purity) under vacuum conditions by bombardment with a high kinetic energy (< 5 keV) and intensity (150 mA) electron beam. The vapour was condensed onto the surface of the substrate (K-βAl_2O_3 pellet) at room temperature in two steps by varying the zenithal angle, α, formed between the perpendicular to the substrate surface and the evaporation direction. Firstly, to provide a good electrical conductivity to the catalyst/working electrode, a fairly compact Cu layer was grown at α = 0º on the K-βAl_2O_3 pellet. The

microstructure of this compact film consisted of adjacent straight nanocolumns perpendicular to the substrate (β = 0º) and an approximate thickness of 0.8 µm. Subsequently, a porous Cu layer with a tilted columnar microstructure was deposited in a similar way than the former but fixing the zenithal evaporation angle at α = 80º. This top layer presented a porosity of around 50 % associated with large void spaces between separated nanocolumns tilted by an angle β ≈ 60º with respect to the perpendicular to the substrate. It was expected that the high porosity of this outer layer favours the catalytic activity of the copper film. The total thickness of the obtained Cu catalyst/working electrode was 1.6 µm approximately, and the final metal loading was 1.08 mg Cu/cm^2 (1.69 x 10^{-5} mol Cu/cm^2). Thus, this novel preparation technique allowed to prepare a suitable copper electrode combining both good electrical and catalytic properties, as shown below. Similar layers were also prepared at different evaporation angles on silicon supports for characterization purposes. More details about the experimental setup employed in the thin catalyst film preparation can be found elsewhere.[41, 42]

The resultant Cu/K-βAl_2O_3/Au electrochemical catalyst was placed into a single pellet, continuous stirred tank reactor (CSTR) where all electrodes were exposed to the same gas atmosphere. Although the Cu film had a high electrical conductivity after its preparation (surface electrical resistance around 8 Ω), prior to the catalytic activity measurements it was subjected to a 25 % H_2 stream (Ar balance) while heating to 280 ºC (ramp of 5 ºC/min) to ensure its complete reduction. The three electrodes (working, counter and reference) were connected to an Autolab PGSTAT320-N potentiostat-galvanostat (Metrohm Autolab) using gold wires (Alfa Aesar, 99.95 % purity). Hence the electrochemical promotion (EPOC) experiments were carried out by varying the applied catalyst potential measured between the working and reference electrodes (V_{WR}) according to the procedure generally used in conventional three-electrodes electrochemical cells.[1]

Electrochemical catalyst characterization

The deposited porous Cu layer was firstly characterized by X-Ray Diffraction (XRD) analysis using a Philips PW-1710 instrument with Cu K_α radiation (λ = 1.5404 Å). The surface and in-depth microstructure of the Cu films deposited on silicon substrates were examined by plan-view and cross-sectional scanning electron microscopy (SEM) analysis using a Hitachi S4800 field emission microscope operated at 2 keV. Given the possibility that the Cu electrode could be oxidized under reaction conditions or damaged by the development of cracks and thus lose its electrical conductivity, the in-plane surface electrical resistance was continuously measured by connecting the catalyst/working electrode to an additional gold wire and a digital multimeter. Cyclic voltammetry was also performed at a scan rate of 5 mV/s with the potentiostat-galvanostat before the EPOC experiments. In this way, a potential range between +1 and -1 V was bounded.

Moreover, the electrochemical catalyst was characterized after the electrochemical promotion experiments. Previously, the Cu catalyst film was exposed to the reaction mixture (CH_3OH/O_2 = 4.4 %/0.3 %) at 320 ºC while applying a negative potential, V_{WR} = -0.5 V in order to electrochemically supply K^+ from the K-βAl_2O_3 pellet to the Cu electrode. After 1 hour, the electrochemical catalyst was cooled down to room temperature under reaction atmosphere. The applied potential was interrupted (open circuit conditions) at 100 ºC. The aim of this procedure was to "freeze out" the catalyst surface conditions pertaining to its electropromoted state. Then the electrochemical catalyst was transferred to different characterization equipments. In first place, the used catalyst film was characterized by XRD to examine the final crystalline structure. SEM was also performed along with Energy-Dispersive X-ray spectroscopy (EDX) elemental mapping analysis by means of a Bruker X-Flash Detector 4010 to identify the surface segregation of different elements. X-ray photoelectron spectra (XPS) were also recorded with a PHOIBOS-100 spectrometer with Delay Line Detector (DLD) from SPECS, which worked in the constant pass energy mode fixed at 30 eV. Monochromatic Mg Kα radiation was used as excitation source and the binding energy (BE) scale of the spectra referenced to the C1s of graphitic carbon taken at 284.6 eV.

Catalytic activity measurements

The catalytic experiments were carried out in an experimental setup employed previously.[14] The reaction gases (Praxair, Inc.) were certified standards (99.999 % purity) of air (as source of O_2 for the methanol partial oxidation reaction), H_2 (reductant agent) and Ar (carrier gas). The gas flow rates were controlled by a set of mass flowmeters (Bronkhorst EL-FLOW) while methanol was fed by sparging Ar through a thermostated saturator containing liquid CH_3OH (Panreac, 99.8 % purity). All lines placed downstream from the saturator were heated above 100 ºC to prevent condensation. Methanol partial oxidation (POM) experiments were carried out at atmospheric pressure with an overall gas flow rate of 6 NL h^{-1}, temperatures from 280 ºC to 360 ºC and a feed composition of CH_3OH/O_2 = 4.4 %/0.3 % (Ar balance). Reactant and product gases were on-line analyzed by using a double channel gas chromatograph (Bruker 450-GC) equipped with Hayesep Q-Molsieve 13X consecutive columns and a CP-Wax 52 CB column, along with thermal conductivity and flame ionization detectors, respectively. The detected reaction products were: H_2, CO_2, H_2O and $HCOOCH_3$ (methyl formate). The error in the carbon atom balance did not exceed 5 %, indicating no consistent loss of material and no significant formation of other oxygenated species.

Results and discussion

Characterization of the Cu catalyst film as-prepared by OAD

Figure 1 shows the X-ray diffractogram of an oblique angle deposited copper film on a silicon substrate at α = 80º. This diffractogram evidences that the as-deposited Cu catalyst film exhibited a well-defined face-centered cubic (FCC) crystalline structure (JCPDS, 89-2838) depicting the (111), (200), (220), (311) and (222) diffraction peaks of copper at 2θ = 43.2º, 50.4º, 74.1º, 89.9º and 95.1º, respectively. A very intense Si(400) peak was also found at 2θ = 69.1º (JCPDS, 35-1241) which corresponded to the substrate.

The microstructure of the Cu layers with different porosities prepared by either normal or oblique evaporation (i.e., OAD) on silicon substrates was characterized by SEM. Figures 2a and 2b show the cross-section and plan-view images, respectively, of the

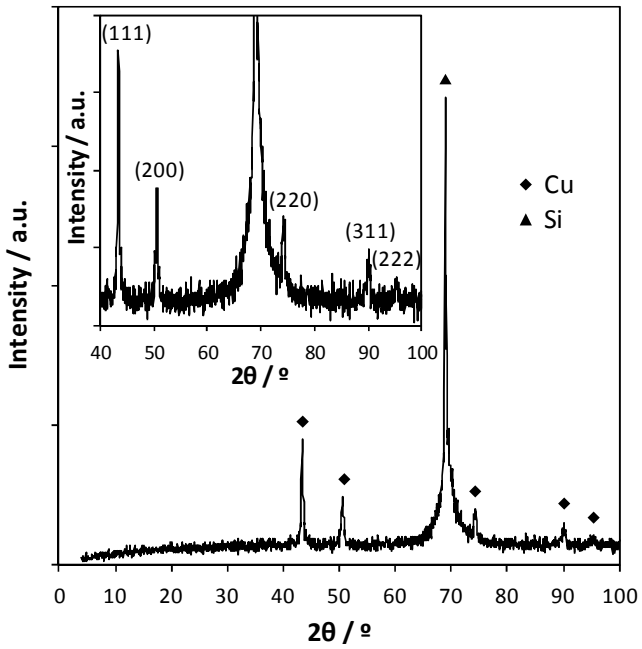

Fig. 1 XRD spectrum of the Cu film as-deposited by OAD on a silicon substrate.

rather compact layer prepared at α = 0º and reveal that it was formed by perpendicular thin and close-packed nanocolumns as expected for metal thin films deposited under the conditions of the zone I of the zone structure model.[43] This first compact Cu layer constituted the inner layer of the copper electrode and provided a very good electrical conductivity (6 – 8 Ω) as well as a high mechanical stability to the electrocatalytic cell. Nevertheless, as observed in the top view of figure 2b, this film presents some diffusion surfaces at the interfacial boundaries of Cu columns which may allow the migration of potassium ions though itself to the gas-exposed Cu catalyst surface. On the other hand, Figures 2c and 2d show the microstructure of the copper layer prepared by OAD at α = 80º. A thickness of around 0.8 µm and a microstructure consisting of tilted and separated nanocolumns with β = 60º can be deduced from the cross section image. The open porosity of this layer, which in practice was extended from the interface with the dense copper underlayer up to the external surface of the catalyst, provided a free access and intimate contact with the reaction gases. Although not all columns presented exactly the same height, a quite uniform nanocolumn cross-sectional diameter of around 120 nm and a column density of the order of 10^9 columns per cm^2 can be also deduced from these images. Similar microstructures obtained by OAD have been reported for a large variety of materials (see for example previous works on Co,[44] Pt-Ni,[33] TiO_2[30, 31, 41] or Ta_2O_5[31, 42] films).

Hence, very interestingly, the OAD technique allowed to deposit metallic films with a suitable porous microstructure for catalytic and electrocatalytic purposes. Herein, an electrode film was developed consisting of a copper compact-porous bilayer (which will be henceforth treated as a single film) that was utilized as an electrochemical catalyst in the POM reaction.

Electrochemical promotion of methanol partial oxidation

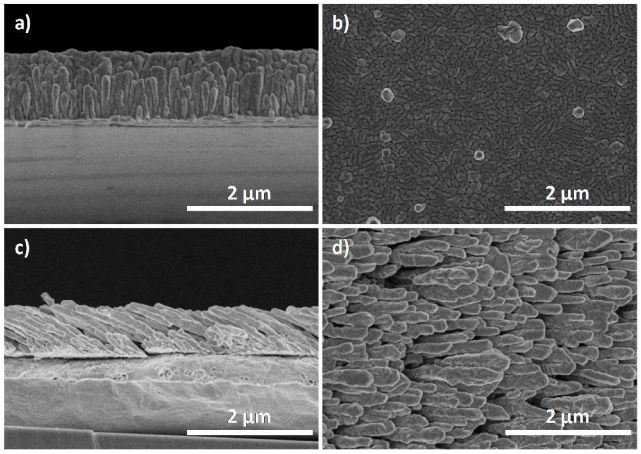

Fig. 2 Cross-sectional and top view SEM images of the Cu films as-prepared on silicon substrate at a normal geometry (a and b, respectively) and at an angle of deposition of 80 º (c and d, respectively). These layers constituted the inner and outer Cu layers at the electrochemical catalyst, respectively.

Influence of the applied potential and reaction mechanism considerations

The Cu/K-βAl_2O_3/Au solid electrolyte cell was tested in the methanol partial oxidation reaction with a feed composition of CH_3OH/O_2 = 4.4 %/0.3 % at 320 ºC in order to study the phenomenon of Electrochemical Promotion of Catalysis (EPOC). A potential interval of ±1 V was selected based on cyclic voltammetry measurements. Figure 3 shows the current (I) variation with the applied potential (V_{WR}) under such reaction conditions during a cyclic voltammetry performed at a quite slow scan rate of 5 mV/s. This voltammogram was found to be very reproducible from the second cycle. A totally null oxidation current was not obtained at +1 V. However, both cathodic (negative) and anodic (positive) scans must be influenced by the charging current associated to the Cu-KβAl_2O_3 interface, which is directly proportional to its capacitance and the scan rate.[45] The most important feature is the appearance of clear cathodic and anodic peaks in the studied potential range, which can be linked to the formation and decomposition of promoter-derived surface compounds, respectively. The integration of both peaks from their respective baselines showed to be quite similar, with a difference of near 10 %. Moreover, this similarity was even higher by considering the positive and negative I vs time curves obtained during the EPOC experiments as will be observed below. This means that a positive potential of 1 V led to the decomposition of practically all the promoter compounds previously formed on the catalyst surface during the cathodic scan. One can find in literature a wide range of positive unpromoted potentials employed in alkali-based electropromoted systems, from +0.1 V[24] or +0.7 V,[40] up to +3 V[12] or +4 V.[27] In the present study, a positive potential of 1 V was selected as lowest possible value to avoid the deterioration of the catalyst film and/or the solid electrolyte, while providing a completely reversible promotional effect.

Figure 4 shows the dynamic response of the reaction rate of the detected products, i.e., hydrogen, carbon dioxide and methyl formate, as well as the current (I) vs. time curves obtained upon the application of different catalyst potentials (V_{WR}) between +1 and -1 V at a temperature of 320 ºC. Each polarization step was

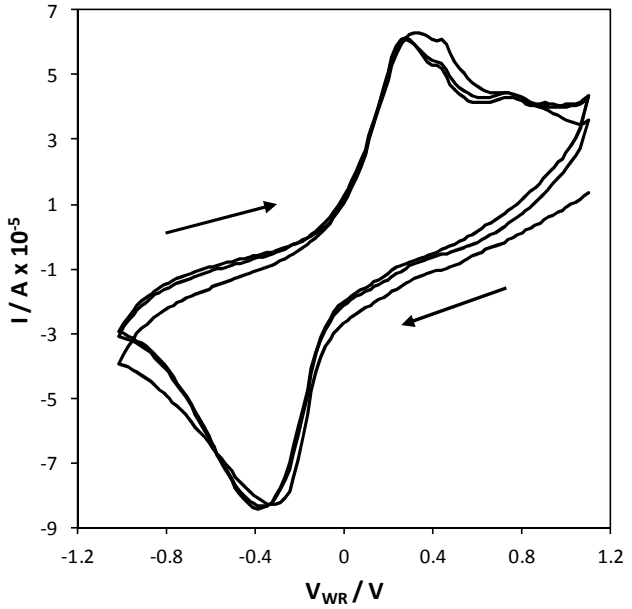

Fig. 3 Current (I) variation vs. the applied potential (VWR) during the cyclic voltammetry between +2 and -2 V (scan rate = 5 mV/s). Methanol partial oxidation conditions: CH_3OH/O_2 = 4.4 %/0.3 %, 320 ºC.

performed for 1 hour to reach a steady-state rate value. Similar to other EPOC studies based on K^+-conductor materials,[12-14, 18, 22, 46, 47] the application of a positive potential (V_{WR} = +1 V) at the beginning of the experiment led to the removal of the potassium promoter from the catalyst/working electrode that could have thermally migrated from the solid electrolyte. In this way, V_{WR} = +1 V was defined as the reference state potential and its imposition before each different polarization allowed to start from the unpromoted state and to check the reversibility and reproducibility of the promotional effect. It can be observed in Figure 4a that under unpromoted conditions the Cu catalyst film already showed certain catalytic activity for the production of hydrogen and carbon dioxide, as well as water (not depicted), from the methanol partial oxidation reaction (eq 1).

$$CH_3OH + ½O_2 \rightarrow 2H_2 + CO_2 \quad (1)$$

Carbon dioxide was the main product obtained in this reference (unpromoted) state. No carbon monoxide was detected but an appreciable amount of methyl formate ($HCOOCH_3$) was also produced. This later compound is a very interesting by-product with many industrial applications; for example, as a precursor in the synthesis of formic acid, formamide and dimethylformamide. The decrease in the applied potential to V_{WR} = +0.5 V caused only a slight increase in H_2 and CO_2 production rates. This potential was close to the open circuit value (V_{WR}^0), which oscillated in the range 0.3-0.5 throughout this entire EPOC study performed at different reaction temperatures. Hence, this first decrease in the applied potential did not constitute a clear negative overpotential nor a significant transfer of potassium species. However, under the application of V_{WR} = 0 V, the reaction rate of all products (H_2, CO_2 and $HCOOCH_3$) sharply increased (electrochemically promoted state), being H_2 the main reaction product. It should be noted that, in this case, the applied potential was already lower than the open circuit potential value leading to the observed negative current values (Figure 4b), i.e.,

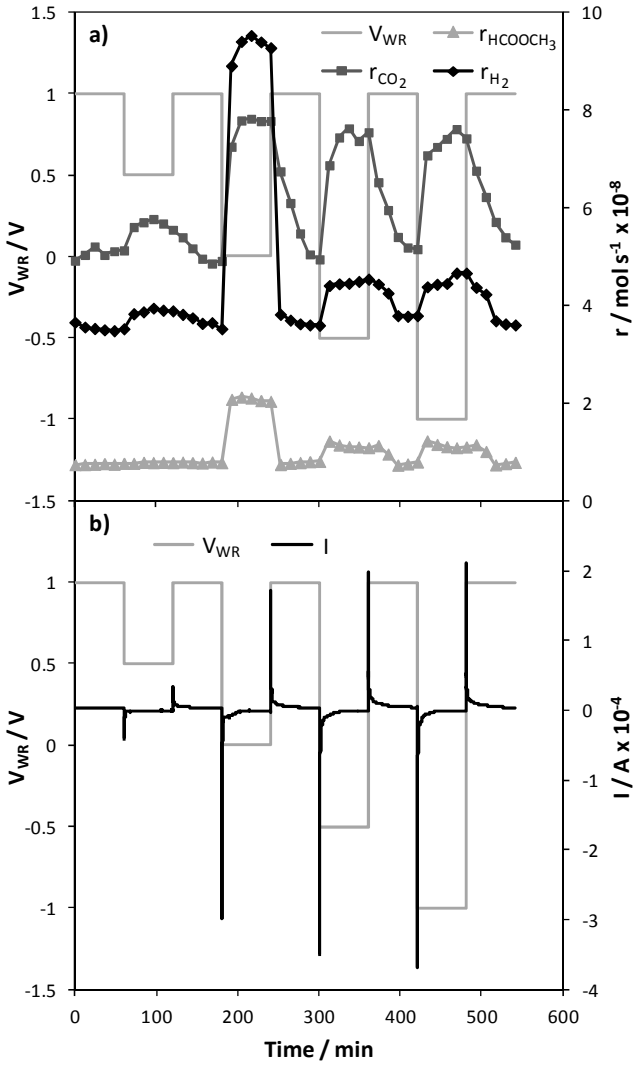

Fig. 4 Response of H_2, CO_2 and $HCOOCH_3$ production rates (a) and obtained electric current (I) (b) vs. time to step changes in the applied catalyst potential (V_{WR}). Methanol partial oxidation conditions: CH_3OH/O_2 = 4.4 %/0.3 %, 320 ºC.

under these conditions, K^+ ions were electrochemically pumped from the K-βAl_2O_3 pellet to the Cu catalyst film. An increase in the alkali concentration on the catalyst surface upon decreasing the applied potential has been previously demonstrated, for instance, by Professor Lambert and co-workers by means of in-situ XP spectroscopy studies on Cu,[24, 25, 40] Pt[48] and Rh.[49] Hence, the observed modification of the Cu catalytic activity with the applied potential can be attributed to a decrease in the catalyst work function, which was a consequence of the migration of electropositive ions leading to a modification of the chemisorptive properties of the Cu surface during the catalytic reaction.[40]

Regarding the reaction mechanism, it is widely accepted that the first reaction step in the methanol oxidation processes is the formation of methoxy species from methanol which is favoured by the presence of surface oxygen through a dissociative adsorption mechanism:[36-38]

$$O_2 + 2* \rightarrow 2O* \quad (2)$$

$$CH_3OH + O^* + * \rightarrow CH_3O^* + OH^* \quad (3)$$

where * denotes a free adsorption site on the catalyst surface. Then, as proposed in an illustrative scheme by Sakong,[38] several consecutive reactions may take place leading to the production of CO_2 (eq 4-6), H_2 (eq 7) and H_2O (eq 8).

$$CH_3O^* + O^* \rightarrow H_2CO^* + OH^* \quad (4)$$

$$H_2CO^* + O^* \rightarrow HCOO^* + H^* \quad (5)$$

$$HCOO^* \rightarrow CO_2 + H^* \quad (6)$$

$$2H^* \rightarrow 2^* + H_2 \quad (7)$$

$$H^* + OH^* \rightarrow H_2O + 2^* \quad (8)$$

On the other hand, the formation of methyl formate can be explained by considering the large set of possible reaction pathways and intermediate species reported elsewhere[36, 39, 50, 51] for the methanol oxidation over Cu-based catalysts. For instance, the following reaction mechanism could be proposed:[51]

$$CH_3O^* + O^* \rightarrow HCOO^* + H_2 + * \quad (9)$$

$$CH_3O^* + HCOO^* \rightarrow HCOOCH_3^* + O^* \quad (10)$$

$$HCOOCH_3^* \rightarrow HCOOCH_3 + * \quad (11)$$

According to the theory of the electrochemical promotion of catalysis,[1] under electropromoted conditions ($V_{WR} \leq 0$ V in this work) the back-spillover of K^+ ions from the solid electrolyte onto the catalyst/working electrode would strengthen the bond between copper and electron-acceptor adsorbates, while it would weaken the bonding with the electron-donor reactants. Under POM conditions, these molecules should be identified as O_2 and CH_3OH, respectively. Hence, the enhancement of the Cu catalytic activity experimentally observed under negative polarization is in good agreement with other POM studies[37] where a positive order of the reaction rate was found with respect to the oxygen partial pressure (for low values). Likewise, an increase in the methanol reaction rate with O_2 concentration was found in previous EPOC studies with different electrochemical catalysts.[52-54] Moreover, this kind of positive promotional effect upon cathodic polarization (electrophilic EPOC behaviour) was also observed over Cu catalysts in other studies on NO reduction by CO[24, 25] and, very recently, on CO_2 hydrogenation under certain reaction conditions.[27] In the present study, the adsorbed oxygen would play an important role by favouring the O-H bond rupture in eq 3. Nevertheless, the rate-limiting step in this kind of process is usually considered the methoxy decomposition (eq 4 and 9).[37, 38] The electrophilic EPOC effect could have also favoured the C-H bond cleavage in the methanol and intermediates decomposition reactions.[53, 54]

It can also be observed in Figure 4a that all the products reaction rates (H_2, CO_2 and $HCOOCH_3$) were restored to their initial values upon every positive polarization at V_{WR} = +1 V. This demonstrates the complete reversibility and reproducibility of the electropromoted effect, as well as the high stability of the Cu electrode along the whole experiment. Moreover, optimal promotional conditions were found at V_{WR} = 0 V. A further decrease of the applied potential down to -0.5 and -1 V led again to an electro-promotional effect. In this case, a less pronounced increase of all the reaction rates with respect to those found under unpromoted conditions occurred, which can be attributed to a detrimental effect of an excess of alkali promoter and the concomitant formation of alkali-derived surface compounds that may partially block catalytic active sites. This is a common effect observed both in EPOC[13, 14, 18, 22, 46, 47] and in conventional alkali chemical promotion studies.[55, 56]

Regarding the possible oxidation of copper during the POM reaction, the in-plane surface electrical resistance was continuously measured leading to values lower than 10 Ω throughout the entire study. As it will be later discussed, these low resistance values would indicate the catalyst/working electrode to mainly remain on its metallic state during the reaction. It should be also mentioned that the methanol conversion obtained in this work (not depicted) did not exceed the 5 %, which was probably influenced by the characteristics of the catalyst, in film form, and thus a still low geometric area. Nevertheless, it is important to stress that both catalytic activity and selectivity of the Cu film in the POM reaction can be in-situ improved under polarization conditions and tuned depending on the applied electric current or potential via electrochemical promotion. This feature of the EPOC phenomenon has been previously shown in other works on POM over alkali-promoted noble metals catalysts.[13, 14] In the present study, the Cu-catalyzed H_2 production was enhanced up to three times at 320 ºC, the H_2 selectivity being increased from 27.4 % (unpromoted conditions, V_{WR} = +1 V) up to 39.1 % (optimum electropromoted conditions, V_{WR} = 0 V). These values were calculated as 100 x mol H_2 / (2 x mol reacted CH_3OH). Moreover, from the integration of the different current vs. time curves, the amount of promoter electrochemically transferred and the promoter to copper ratio (θ_{K+}) can be estimated at each applied potential through the following equations:

$$\text{Promoter supply / mol } K^+ = \int_0^t \frac{|I|}{n\,F}\,dt \quad (12)$$

$$\theta_{K^+} = \frac{\int_0^t \frac{|I|}{n\,F}dt}{N} \quad (13)$$

where n is +1 in this case, F is the Faraday constant ($96485\ C\ mol_e^{-1}$), t is the polarization time and N is the total amount of Cu deposited (3.4 x 10^{-5} mol Cu). This parameter was estimated in this way due to the difficulty of calculating the Cu active sites in this electrocatalytic system. The potassium to copper ratio varied from 1 x 10^{-3} (at V_{WR} = +0.5 V) to 8.5 x 10^{-3} (at V_{WR} = -1 V). Hence, the EPOC phenomenon allows to determine the optimum promoter to copper ratio ($\theta_{K+,opt}$) which leads to the maximum reaction rate. In this study, this value is $\theta_{K+,opt}$ = 6.3 x 10^{-3}, obtained at V_{WR} = 0 V.

Influence of the reaction temperature

The influence of the reaction temperature on the copper catalytic activity was studied at a fix feed composition (CH_3OH/O_2 = 4.4 %/0.3 %) and different applied potentials. Figure 5 shows the variation of the steady-state reaction rates of the different products vs. the applied catalyst potential at different reaction temperatures between 280 and 360 ºC. In order to quantify the magnitude of the electropromotional effect, the maximum rate enhancement ratios (ρ_{max}) for the optimum applied potential are also included in the figure. This parameter was calculated with

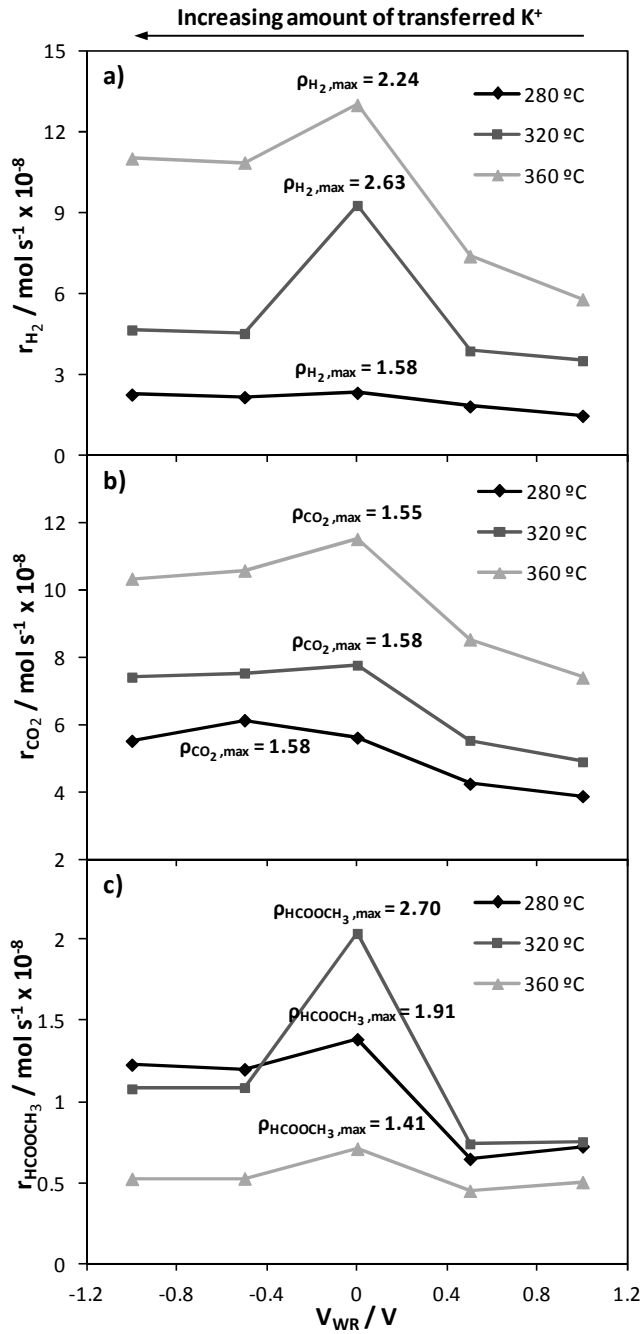

Fig. 5 Steady-state H_2 (a), CO_2 (b) and $HCOOCH_3$ (c) production rates vs. the applied potential (V_{WR}) as well as the corresponding maximum production rates enhancement ratios (ρ_{max}) at different reaction temperatures (280-360 ºC). Methanol partial oxidation conditions: CH_3OH/O_2 = 4.4 %/0.3 %.

the following equation:

$$\rho_i = \frac{r_i}{r_{i,0}} \quad (14)$$

where, for each compound, r_i and $r_{i,0}$ are the promoted (V_{WR} < +0.5 V) and unpromoted (V_{WR} = +1 V) catalytic production rates, respectively.

Starting from the reference unpromoted state (V_{WR} = +1 V) and according to the previous considerations, the decrease in the applied potential caused the electrochemical pumping of K^+ ions

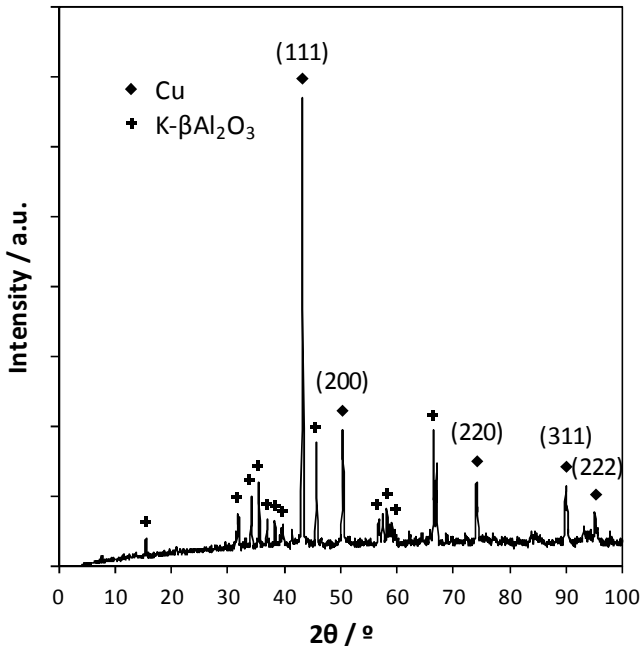

Fig. 6 XRD diffractogram of the electrochemical catalyst after the EPOC experiments (320 ºC, CH_3OH/O_2 = 4.4 %/0.3 %, V_{WR} = -0.5 V for 1 h).

from the solid electrolyte to the Cu catalyst film. As a result, at the three studied temperatures, all the products reaction rates (H_2, CO_2, $HCOOCH_3$) increased because of the potassium promotional effect, evidencing an electrophilic EPOC behavior ($\Delta r > 0$, $\rho > 1$, upon negative polarization).[1] It should be noted that at every reaction temperature, the same operational procedure was carried out than in the experiment shown previously (Figure 4), i.e., a potential of +1 V was applied at the end of every experiment and before each different applied potential. In this way, both the reversibility and the reproducibility of the electropromotional effect were verified at all the reaction temperatures, as well as the stability of the catalytic activity confirmed throughout the entire study.

Under unpromoted conditions (V_{WR} = +1 V), the Cu catalytic activity increased with the reaction temperature in good agreement with other POM studies over conventional Cu supported catalysts (e.g., Cu/ZnO,[37] $Cu/ZnO/Al_2O_3$[39, 50] or Cu/ZrO_2[35]). As an exception, a decrease in the methyl formate production rate was found at the highest temperature (360 ºC), which can be attributed to its decomposition or further oxidation to CO_2 as reported in other works with Cu-based catalysts.[39, 50, 51] Meanwhile, under optimum electropromoted conditions (V_{WR} = 0 V), an increase in both the H_2 and $HCOOCH_3$ production rate enhancement ratios (ρ) was found when increasing the temperature from 280 to 320 ºC, due to an increase in both the copper catalytic activity and the solid electrolyte ionic conductivity at fixed potential. The less pronounced EPOC effect found at 360 ºC should be likely related with the higher unpromoted reaction rate (r_0). Moreover, in line with experiment in Figure 4, a possible poisoning effect by potassium-derived surface compounds can be observed under the application of the lowest applied potentials (V_{WR} = -0.5 and -1 V).

These POM results at different temperatures showed that the catalytic performance of this novel Cu film prepared by OAD can be enhanced in a controlled and reversible way via alkaline

Cite this: DOI: 10.1039/c0xx00000x

www.rsc.org/xxxxxx

ARTICLE TYPE

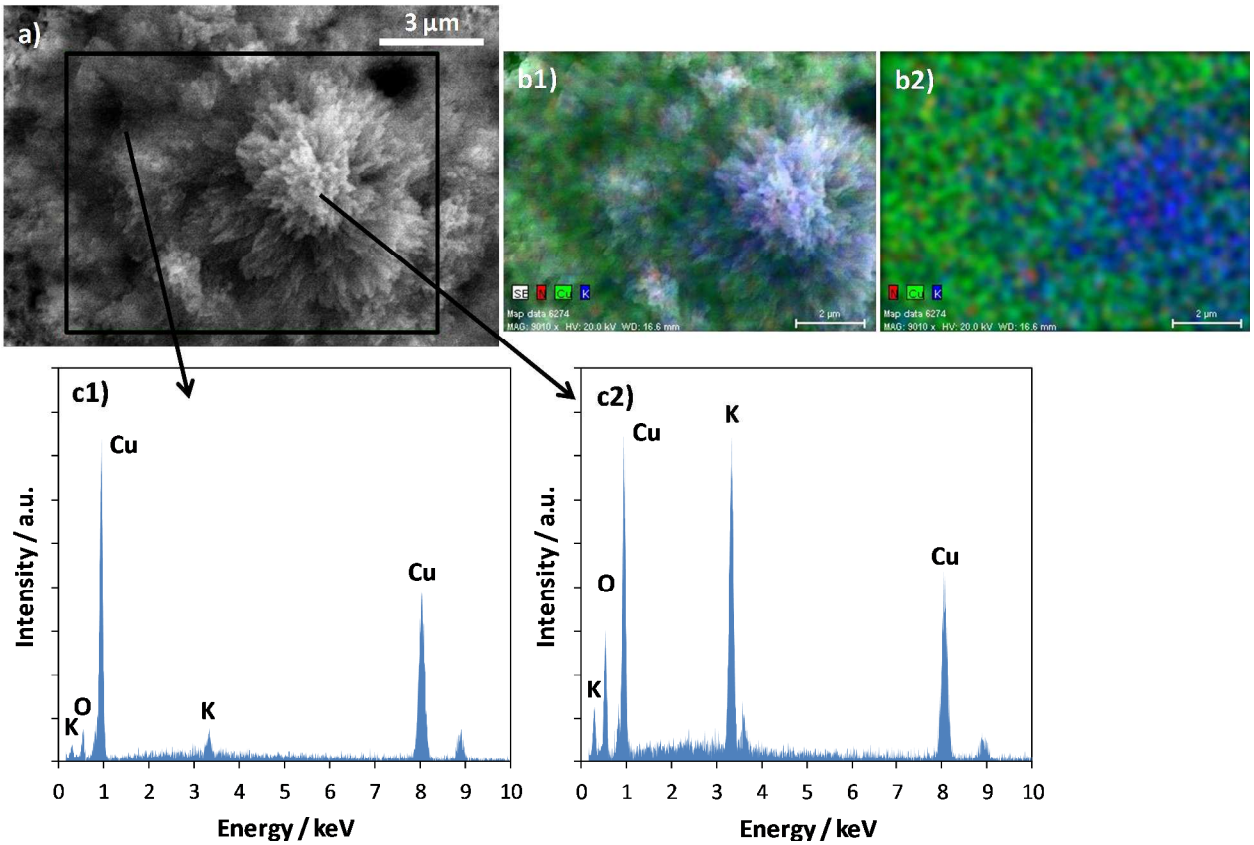

Fig. 7 Top view SEM image of a selected area of the electrochemical catalyst (a) after the EPOC experiments (320 ºC, CH_3OH/O_2 = 4.4 %/0.3 %, V_{WR} = -0.5 V for 1 h), along with the corresponding elemental mapping (b1 and b2) of Cu (green), K (blue) and N (red) and the EDX spectra from different regions (c1 and c2).

electrochemical promotion. Under optimal reaction conditions (320 ºC, V_{WR} = 0 V), the hydrogen and methyl formate production rates increased by 2.63 and 2.70 times, respectively. It must be stressed that this maximum enhancement of the H_2 production rate ($\rho_{H_2,max} = 2.63$) was higher, for instance, than that previously obtained in other EPOC study ($i.e., \rho_{H_2,max} = 1.63$) with an electrochemical catalyst based on platinum nanoparticles (0.014 mg Pt/cm^2) and similar methanol partial oxidation conditions (320 ºC and O_2/CH_3OH = 0.08) [13]. Therefore, these results show that under the explored reaction conditions a non-noble metal catalyst (such as Cu) can be electrochemically activated in a similar or even more pronounced way than a noble metal catalyst such as Pt. This way, one can suggest that EPOC phenomena could be used to increase the catalytic activity of a non-noble metal up to the typically higher activity of a noble metal, for example, in H_2 production processes.

Post-reaction characterization of the electrochemically promoted Cu catalyst

In first place, it should be noted that the reaction rates observed under the last two potentiostatic transitions at 320 ºC (before the post-reaction characterization), i.e. +2 and -0.5 V, were very similar to those obtained during the first experiment performed at 320 ºC (Figure 4). This verifies the good reproducibility of Cu catalytic activity even after heating up to 360 ºC. The XRD spectra of the used catalyst film after the EPOC experiments is shown in Figure 6. It presents five diffraction peaks corresponding to the typical face-centered cubic structure (JCPDS, 89-2838) of metallic copper. An average Cu particle size (d) of 43 nm can be estimated from the width of the main diffraction peak, Cu(111), by means of the Scherrer formula. Peaks associated with the K-βAl_2O_3 pellet (JCPDS, 21-618) can also be observed. No diffraction peaks related to potassium compounds like carbonates or bicarbonates were found. Neither diffraction peaks associated with copper oxides like CuO nor Cu_2O were detected. However, the minority presence of these compounds cannot be ruled out because some overlapping may take place with the peaks of alumina, for instance, in the case of the CuO peak at 2θ = 35.4º (JCPDS, 80-1917).

Figure 7 shows the SEM micrograph of a selected region of the catalyst-electrode where highly grown surface crystals were observed. Its corresponding elemental mapping and spectra by

Cite this: DOI: 10.1039/c0xx00000x

www.rsc.org/xxxxxx

ARTICLE TYPE

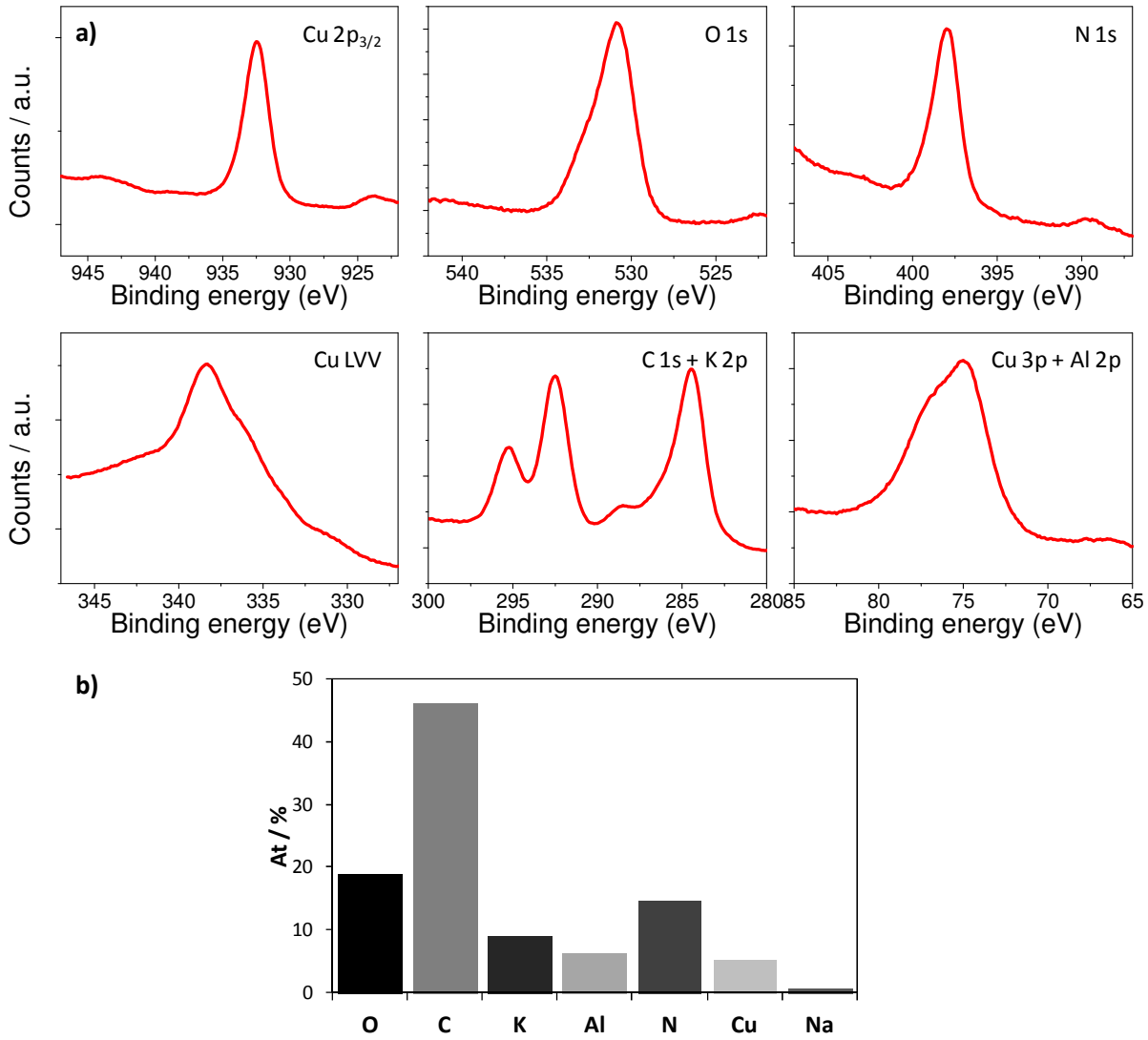

Fig. 8 XPS spectra of the electrochemical catalyst after the EPOC experiments (320 ºC, CH_3OH/O_2 = 4.4 %/0.3 %, V_{WR} = -0.5 V for 1 h). Spectra taken at different binding energy regions to show the presence of the different elements present on the surface of the sample (a). The corresponding surface atomic composition expressed in percentages (b).

EDX are also reported. The columnar structure observed in Fig. 2 seems to disappear in this figure, although both micrographs were not carried out under exactly the same operation conditions. In the case of some morphology change, the most feasible reason would be certain Cu sintering that could take place during the experiment at high temperature (360 ºC).[57] However, the catalyst porosity seemed to be preserved. In fact, the reversibility and reproducibility of both the catalyst activity and the promotional effect were verified in the whole temperature range studied (Figure 4 and 5), also after cooling from 360 ºC. As previously highlighted, the catalyst showed the same unpromoted catalytic activity after several working hours. In Figures 7b1 and 7b2, large concentrations of potassium (in blue) were found on certain areas of the Cu surface (in green). This seems to indicate that some potassium-derived surface compounds were formed on the Cu surface during the EPOC experiments and might block Cu active sites causing the decrease in the reaction rates observed in Figures 4 and 5 under the application of high negative potentials. Under our working conditions, the most feasible K-derived surface compounds are potassium oxides and/or carbonates formed by reaction with O_2, H_2O and carbon-containing molecules in the reaction mixture. These types of compounds were previously found over other metal catalysts such as Rh,[58] Pt[47] or Ag,[46] and may be obtained, for instance, through the following electrocatalytic reactions:

$$2K^+ + ½O_2 + 2e^- \rightarrow K_2O \quad (15)$$

$$2K^+ + ½O_2 + CO_2 + 2e^- \rightarrow K_2CO_3 \quad (16)$$

Although the potassium distribution along the catalyst thickness was not studied, it was important to demonstrate that K^+ ions were able to migrate through the catalyst film and reach the outermost surface. The presence of potassium compounds was also revealed by EDX analysis taken in different areas of the micrograph. Figure 7c2 shows that the K and O signals were much higher in the spectra taken in the agglomerates than those from the flat region (Figure 7c1). Moreover, it is also worth noting that nitrogen (red points) was found uniformly distributed on the film surface. This elemental nitrogen can only proceed from the fed air stream, and its presence on the catalyst surface will be confirmed and further discussed by XPS analysis.

The chemical state and composition of the outer surface layers of the Cu catalyst were studied by XPS. The Cu2p photoemission (BE = 932.4 eV) and Cu LVV Auger (kinetic energy 915.14 eV) spectra obtained (Figure 8a) can be used to determine the Auger parameter of copper (AP = BE photoemission peak + kinetic energy Auger peak) which presented a value of 1847.54 eV, typical of Cu^{+}[59] (neither Cu^0 nor Cu^{2+}). This finding would agree with previous results in the sense that the Cu active state in the methanol partial oxidation reaction could be considered Cu^+.[50] However, it should be noted that the XPS characterization is only sensitive to a surface thickness of a few nanometers and that, therefore, the Cu_2O observed at the outermost catalyst layer could also be attributed, at least in part, to the exposure of the sample to the air atmosphere during its transfer from the reaction cell to the characterization equipment. An oxidation limited to the outermost surface layers agrees with the very low surface electrical resistance (below 10 ohms) and the XRD analysis of the utilized catalyst that should remain mainly as metallic copper under the studied reaction conditions. On the other hand, the N1s peak observed at 398 eV demonstrated the presence of some reduced nitrogen on the catalyst surface, probably derived from a certain K-promoted interaction between nitrogen from air and produced hydrogen. It is well known that ammonia synthesis is typically promoted by potassium.[56] Furthermore, ammonia synthesis reaction has been electrochemically promoted by H^+ ions in previous studies with Fe catalysts under both high pressure[4] and atmospheric pressure.[23] The C1s signal in the spectrum of the used sample also shows the presence of surface carbon mostly in the form of graphitic or hydrogenated carbon. This indicates that a certain coking could have taken place at the highest reaction temperatures. However, at least part of the O, C and K amounts observed in this figure can be associated to promoter derived species as previously mentioned. The aluminium also found in this XPS spectrum can be attributed to some uncovered regions of the K-βAl_2O_3 electrolyte which might have appeared due to small scratches caused by the contact with the gold wires. A quantitative estimation of the elemental concentration in the examined outer layer of the utilized electrocatalyst is also included in Figure 8b.

Conclusions

From the previous results and discussion, we can conclude that the OAD technique is a straightforward method to prepare a kind of novel Cu catalytic films with a tuneable microstructure. Combining the physical vapour deposition at normal and oblique angles for the fabrication of a bilayer film has yielded a catalytic layer with both a high surface electrical conductivity and a high porosity (around 50 %), very suitable for catalytic and electrocatalytic applications.

In this study we have also shown that a non-noble catalyst can be electrochemically activated in the partial oxidation of methanol. The catalytic activity of the Cu electrode was enhanced by electrochemically supplying of K^+ ions in a controlled, reversible and reproducible way. The observed promotional effect can be explained according to the rules of chemical/electrochemical promotion.

Under electrochemical promotion conditions, potassium-derived compounds were formed on the Cu catalyst surface as determined by post-reaction EDX and XPS characterization. The formation of some adsorbed nitrogen functional groups also seemed to take place under the promotional effect of potassium due to the presence of N_2 and H_2 in the reaction atmosphere.

Acknowledgments

We gratefully acknowledge Spanish Ministry of Economy and Competiveness (projects MAT2013-40852-R, MAT2013-42900-P and CTQ2013-45030-R) for the financial support of this work.

Notes and references

[a] *Department of Chemical Engineering, School of Chemical Sciences and Technology, University of Castilla-La Mancha, Avda. Camilo José Cela 12, 13005 Ciudad Real, Spain.*
[b] *Laboratory of Nanotechnology on Surface, Institute of Materials Science of Sevilla (CSIC-Uni. Sevilla), Avda. Américo Vespucio 49, 41092 Sevilla, Spain.*
** Corresponding author: Fax: +34-926295437; Tel: 34-926295300; E-mail: Antonio.lconsuegra@uclm.es*

1. C.G. Vayenas, S. Bebelis, C. Pliangos, S. Brosda and D. Tsiplakides, *Electrochemical Activation of Catalysis: Promotion, Electrochemical Promotion and Metal-Support Interactions*, Kluwer Academic Publishers/Plenum Press, New York, 2001.
2. A. de Lucas-Consuegra, *Catalysis Surveys from Asia*, 2014, in press.
3. P. Vernoux, L. Lizarraga, M. N. Tsampas, F. M. Sapountzi, A. De Lucas-Consuegra, J. L. Valverde, S. Souentie, C. G. Vayenas, D. Tsiplakides, S. Balomenou and E. A. Baranova, *Chemical Reviews*, 2013, 113, 8192-8260.
4. C. G. Yiokari, G. E. Pitselis, D. G. Polydoros, A. D. Katsaounis and C. G. Vayenas, *Journal of Physical Chemistry A*, 2000, 104, 10600-10602.
5. S. Balomenou, D. Tsiplakides, A. Katsaounis, S. Thiemann-Handler, B. Cramer, G. Foti, C. Comninellis and C. G. Vayenas, *Applied Catalysis B: Environmental*, 2004, 52, 181-196.
6. S. Souentie, A. Hammad, S. Brosda, G. Foti and C. G. Vayenas, *Journal of Applied Electrochemistry*, 2008, 38, 1159-1170.
7. E. I. Papaioannou, S. Souentie, A. Hammad and C. G. Vayenas, *Catalysis Today*, 2009, 146, 336-344.
8. D. Poulidi, M. E. Rivas, B. Zydorczak, Z. Wu, K. Li and I. S. Metcalfe, *Solid State Ionics*, 2012, 225, 382-385.
9. M. Marwood and C. G. Vayenas, *Journal of Catalysis*, 1998, 178, 429-440.
10. A. Kambolis, L. Lizarraga, M. N. Tsampas, L. Burel, M. Rieu, J. P. Viricelle and P. Vernoux, *Electrochemistry Communications*, 2012, 19, 5-8.
11. V. Jiménez, C. Jiménez-Borja, P. Sánchez, A. Romero, E. I. Papaioannou, D. Theleritis, S. Souentie, S. Brosda and J. L. Valverde, *Applied Catalysis B: Environmental*, 2011, 107, 210-220.

12. A. de Lucas-Consuegra, A. Princivalle, A. Caravaca, F. Dorado, A. Marouf, C. Guizard, J. L. Valverde and P. Vernoux, *Applied Catalysis A: General*, 2009, 365, 274-280.
13. A. de Lucas-Consuegra, J. González-Cobos, V. Carcelén, C. Magén, J.L. Endrino and J. L. Valverde, *Journal of Catalysis*, 2013, 307, 18-26.
14. J. González-Cobos, D. Horwat, J. Ghanbaja, J. L. Valverde and A. De Lucas-Consuegra, *Journal of Catalysis*, 2014, 317, 293-302.
15. A. Lintanf, E. Djurado and P. Vernoux, *Solid State Ionics*, 2008, 178, 1998-2008.
16. V. Roche, R. Revel and P. Vernoux, *Catalysis Communications*, 2010, 11, 1076-1080.
17. A. De Lucas-Consuegra, A. Caravaca, P. J. Martínez, J. L. Endrino, F. Dorado and J. L. Valverde, *Journal of Catalysis*, 2010, 274, 251-258.
18. A. De Lucas-Consuegra, A. Caravaca, J. González-Cobos, J. L. Valverde and F. Dorado, *Catalysis Communications*, 2011, 15, 6-9.
19. T. I. Politova, V. A. Sobyanin and V. D. Belyaev, *Reaction Kinetics & Catalysis Letters*, 1990, 41, 321-326.
20. I. V. Yentekakis, Y. Jiang, S. Neophytides, S. Bebelis and C. G. Vayenas, *Ionics*, 1995, 1, 491-498.
21. E. Ruiz, D. Cillero, P. J. Martínez, Á. Morales, G. S. Vicente, G. De Diego and J. M. Sánchez, *Journal of CO2 Utilization*, 2014, 8, 1-20.
22. G. E. Pitselis, P. D. Petrolekas and C. G. Vayenas, *Ionics*, 1997, 3, 110-116.
23. M. Ouzounidou, A. Skodra, C. Kokkofitis and M. Stoukides, *Solid State Ionics*, 2007, 178, 153-159.
24. F.J. Williams, A. Palermo, M.S. Tikhov and R. M. Lambert, *Journal of Physical Chemistry B*, 1999, 103, 9960-9966.
25. R.M. Lambert, F. Williams, A. Palermo and M. S. Tikhov, *Topics in Catalysis*, 2000, 13, 91-98.
26. F. M. Sapountzi, M. N. Tsampas and C. G. Vayenas, *Catalysis Today*, 2007, 127, 295-303.
27. E. Ruiz, D. Cillero, P. J. Martínez, Á. Morales, G. S. Vicente, G. De Diego and J. M. Sánchez, *Catalysis Today*, 2014, 236, 108-120.
28. E. Mutoro, C. Koutsodontis, B. Luerssen, S. Brosda, C. G. Vayenas and J. Janek, *Applied Catalysis B: Environmental*, 2010, 100, 328-337.
29. M. Matthew, M. T. Hawkeye and M. J. B. Taschuk, *Glancing Angle Deposition of Thin Films: Engineering the Nanoscale*, Wiley, 2014.
30. M. Oliveros, L. González-García, V. Mugnaini, F. Yubero, N. Roques, J. Veciana, A. R. González-Elipe and C. Rovira, *Langmuir*, 2011, 27, 5098-5106.
31. J. R. Sánchez-Valencia, A. Borrás, A. Barranco, V. J. Rico, J. P. Espinos and A. R. González-Elipe, *Langmuir*, 2008, 24, 9460-9469.
32. Y. He, J. Fan and Y. Zhao, *International Journal of Hydrogen Energy*, 2010, 35, 4162-4170.
33. N. N. Kariuki, W. J. Khudhayer, T. Karabacak and D. J. Myers, *ACS Catalysis*, 2013, 3, 3123-3132.
34. S. A. Francis, R. T. Tucker, M. J. Brett and S. H. Bergens, *Journal of Power Sources*, 2013, 222, 533-541.
35. H. Chen, A. Yin, X. Guo, W. L. Dai and K. N. Fan, *Catalysis Letters*, 2009, 131, 632-642.
36. S. T. Yong, C. W. Ooi, S. P. Chai and X. S. Wu, *International Journal of Hydrogen Energy*, 2013, 38, 9541-9552.
37. L. A. Espinosa, R. M. Lago, M. A. Peña and J. L. G. Fierro, *Topics in Catalysis*, 2003, 22, 245-251.
38. S. Sakong and A. Gross, *Journal of Physical Chemistry A*, 2007, 111, 8814-8822.
39. R. M. Navarro, M. A. Peña and J. L. G. Fierro, *Journal of Catalysis*, 2002, 212, 112-118.
40. F.J. Williams, A. Palermo, M.S. Tikhov and R. M. Lambert, *Journal of Physical Chemistry B*, 2000, 104, 615-621.
41. V. Rico, P. Romero, J. L. Hueso, J. P. Espinós and A. R. González-Elipe, *Catalysis Today*, 2009, 143, 347-354.
42. V. Rico, A. Borrás, F. Yubero, J. P. Espinós, F. Frutos and A. R. González-Elipe, *Journal of Physical Chemistry C*, 2009, 113, 3775-3784.
43. J. A. Thornton, *J Vac Sci Technol*, 1974, 11, 666-670.
44. D. X. Ye, Y. P. Zhao, G. R. Yang, Y. G. Zhao, G. C. Wang and T. M. Lu, *Nanotechnology*, 2002, 13, 615-618.
45. L. R. F. A.J. Bard, *Electrochemical Methods. Fundamentals and Applications*, John Wiley & Sons, New York, 2001.
46. A. Palermo, A. Husain, M. S. Tikhov and R. M. Lambert, *Journal of Catalysis*, 2002, 207, 331-340.
47. A. de Lucas-Consuegra, F. Dorado, J. L. Valverde, R. Karoum and P. Vernoux, *Journal of Catalysis*, 2007, 251, 474-484.
48. I. V. Yentekakis, A. Palermo, N. C. Filkin, M. S. Tikhov and R. M. Lambert, *Journal of Physical Chemistry B*, 1997, 101, 3759-3768.
49. F. J. Williams, A. Palermo, M. S. Tikhov and R. M. Lambert, *Journal of Physical Chemistry B*, 2000, 104, 11883-11890.
50. Y. Choi and H. G. Stenger, *Applied Catalysis B: Environmental*, 2002, 38, 259-269.
51. V. A. Matyshak, O. N. Sil'Chenkova, I. T. Ismailov and V. F. Tret'Yakov, *Kinetics and Catalysis*, 2009, 50, 784-792.
52. A. de Lucas-Consuegra, J. González-Cobos, Y. García-Rodríguez, A. Mosquera, J.L. Endrino and J. L. Valverde, *J. Catal.*, 2012, 293, 149-157.
53. C. G. Vayenas and S. Neophytides, *Journal of Catalysis*, 1991, 127, 645-664.
54. J. K. Hong, I. H. Oh, S. A. Hong and W. Y. Lee, *Journal of Catalysis*, 1996, 163, 95-105.
55. I. V. Yentekakis, M. Konsolakis, R. M. Lambert, N. MacLeod and L. Nalbantian, *Applied Catalysis B: Environmental*, 1999, 22, 123-133.
56. B. Lin, K. Wei, X. Ma, J. Lin and J. Ni, *Catalysis Science and Technology*, 2013, 3, 1367-1374.
57. R. Hughes, *Deactivation of catalysts*, Academic Press, New York, 1984.
58. A. J. Urquhart, J. M. Keel, F. J. Williams and R. M. Lambert, *Journal of Physical Chemistry B*, 2003, 107, 10591-10597.
59. J. P. Espinós, J. Morales, A. Barranco, A. Caballero, J. P. Holgado and A. R. González-Elipe, *Journal of Physical Chemistry B*, 2002, 106, 6921-6929.